Published in final edited form as:
J Mol Biol. 2010 April 2; 397(3): 677–688. doi:10.1016/j.jmb.2010.01.068.

Structural Energetics of the Adenine Tract from an Intrinsic Transcription Terminator

Yuegao Huang, **Xiaoli Weng**, and **Irina M. Russu***
Department of Chemistry and Molecular Biophysics Program, Wesleyan University, Middletown, CT 06459

Abstract

Intrinsic transcription termination sites generally contain a tract of adenines in the DNA template that yields a tract of uracils at the 3'- end of the nascent RNA. To understand how this base sequence contributes to termination of transcription, we have investigated two nucleic acid structures. The first is the RNA-DNA hybrid that contains the uracil tract 5'-rUUUUUAU-3' from the tR2 intrinsic terminator of bacteriophage λ. The second is the homologous DNA-DNA duplex that contains the adenine tract 5'-dATAAAAA-3'. This duplex is present at the tR2 site when the DNA is not transcribed. The opening and the stability of each rU-dA/dT-dA base pair in the two structures are characterized by imino proton exchange and nuclear magnetic resonance spectroscopy. The results reveal concerted opening of the central rU-dA base pairs in the RNA-DNA hybrid. Furthermore, the stability profile of the adenine tract in the RNA-DNA hybrid is very different from that of the tract in the template DNA-DNA duplex. In the RNA-DNA hybrid, the stabilities of rU-dA base pairs range from 4.3 to 6.5 kcal/mol (at 10°C). The sites of lowest stability are identified at the central positions of the tract. In the template DNA-DNA duplex, the dT-dA base pairs are more stable than the corresponding rU-dA base pairs in the hybrid by 0.9 to 4.6 kcal/mol and, in contrast to the RNA-DNA hybrid, the central base pairs have the highest stability. These results suggest that the central rU-dA/dT-dA base pairs in the adenine tract make the largest energetic contributions to transcription termination by promoting both, the dissociation of the RNA transcript and the closing of the transcription bubble. The results also suggest that the high stability of dT-dA base pairs in the DNA provides a signal for the pausing of RNA polymerase at the termination site.

Keywords

Intrinsic transcription termination; base-pair opening; RNA-DNA hybrids; adenine tracts; proton exchange

Introduction

Transcription is the first step in gene expression. The transfer of base sequence information from the DNA to the nascent messenger RNA occurs through a transient RNA-DNA hybrid

*Corresponding author. irussu@wesleyan.edu. Postal address: 203 Hall-Atwater laboratories, Wesleyan University, Middletown, CT 06459. Telephone: (860)-685-2428. Fax: (860)-685-2211.

structure in which RNA bases form complementary pairs with bases in the DNA template strand. The hybrid generally contains 7-9 base pairs.[1, 2] Its formation requires separation of the two DNA strands, through at least 12 base pairs, into a transcription bubble. The transcription process is initiated by binding of RNA polymerase to the promoter of the corresponding gene(s). During the subsequent RNA synthesis, the polymerase remains bound to the DNA and to the nascent RNA. This elongation complex maintains its high stability as it advances through thousands of base pairs at speeds up to 100 base pairs/s. The stability of the complex is, however, lost at the DNA sites where transcription must end. At these sites, the elongation complex disassembles by the release of the RNA transcript and the dissociation of the polymerase from DNA. Transcription termination sites are mostly found at the end of operons.[3] They are also present near promoters and between genes in an operon. In the latter case, the termination sites function as regulators of gene expression: they dictate whether or not transcription of the downstream genes will occur.

In prokaryotes, transcription termination sites are generally classified according to their requirements. Factor-dependent (or Rho-dependent) sites require auxiliary factors, such as Rho protein, to terminate transcription *in vitro*. In contrast, at intrinsic (or Rho-independent) sites, termination is triggered solely by signals encoded in the base sequence and in the structure of the RNA and DNA. In *E. Coli*, about half of the transcription termination sites belongs to this class.[3]

Intrinsic transcription termination sites share two base sequence motifs: a dGC-rich sequence with hyphenated inverted symmetry and a dA-rich tract in the DNA template strand (Figure 1a).[4] The two motifs work in concert with each other to induce termination.[5-10] The GC-rich sequence acts in the RNA transcript where it forms a hairpin. The hairpin disrupts the hybrid downstream from it and alters key contacts of the RNA polymerase with the nucleic acid framework. The second motif exerts its action through the RNA-DNA hybrid. When the polymerase reaches the termination point, the hybrid generated by the dA-rich tract consists of consecutive rU-dA base pairs. Such hybrids are very unstable, as demonstrated previously by optical melting experiments.[11] The instability of the hybrid weakens the conformational constraints for the upstream formation of the hairpin and allows for ready release of the RNA transcript.

Our laboratory has been working toward defining the energetic contributions of individual base pairs from the RNA transcript and the DNA template to the destabilization of the elongation complex at transcription termination sites. The system studied is the tR2 terminator of bacteriophage λ shown in Figure 1. This terminator has been a model system for investigations of the molecular mechanisms of intrinsic transcription termination.[5, 8, 10, 12] The methods of choice in our work are nuclear magnetic resonance (NMR) spectroscopy and proton exchange. The combined use of these two techniques allows us to define the stability of each base pair in several structural states of the nucleic acid framework involved in termination of transcription at the λ tR2 site. In a previous paper, we have reported the structural energetic maps for the two homologous RNA-DNA hybrids formed by the GC-rich sequence.[13] In the present work we report our results on the RNA-DNA hybrid formed when the dA-rich tract is transcribed, and on the homologous DNA-DNA duplex present in the template when the DNA is not transcribed. The RNA-DNA hybrid investigated, henceforth-abbreviated rU-dA RNA-DNA hybrid, is shown in Figure 1b. The main interest of the work is on the rU-dA base pairs of the molecule, which reproduce the hybrid formed at the tR2 site just before the termination point (Figure 1a). The rG-dC/rC-dG base pairs are added at the ends of the duplex to increase the stability of the structure and to prevent the effects of fraying upon proton exchange in the rU-dA base pairs of interest, while maintaining the base sequence context upstream from the hybrid.

Results

Assignment of the Imino Proton Resonances in the rU-dA RNA-DNA Hybrid

Characterization of the stabilities of individual base pairs in nucleic acid structures by NMR spectroscopy relies upon observation of the imino proton in each base pair (Methods section and Figure 1c). The NMR resonances of the imino protons in the rU-dA RNA-DNA hybrid investigated are shown in Figure 2. The spectrum exhibits severe overlap especially for the resonances of rU-dA base pairs, which are of interest in the present work. Due to this overlap, the methods generally used for resonance assignments, such as ^{1}H-^{1}H NOESY, are of limited value in this case. To circumvent this problem, and assign the uracil imino proton resonances, we have constructed RNA-DNA hybrid molecules in which the N3 atom of single uracil bases was ^{15}N-labeled. The ^{15}N-labeled uracil was placed at each of the following positions: 5, 6, 7, 8, 9, and 11. The ^{15}N-edited spectra of these six singly labeled hybrids are shown in Figure 3. As one can see, the resonance of $(rU\text{-}dA)_5$ is the only uracil resonance that is resolved (14.14 ppm). The imino proton resonances of $(rU\text{-}dA)_6$ and $(rU\text{-}dA)_{11}$ both occur at 13.95 ppm, while those of $(rU\text{-}dA)_7$ and $(rU\text{-}dA)_8$ occur at 13.88 ppm. The resonance of $(rU\text{-}dA)_9$ is at 13.12 ppm and, in the unedited spectrum, overlaps with other imino proton resonances (Figure 2).

The imino proton resonances of $(rA\text{-}dT)_{10}$ and of guanines were assigned from ^{1}H-^{1}H NOESY and from uniform ^{15}N-labeling, as detailed in the Supplementary Data.

Imino Proton Exchange in the rU-dA RNA-DNA Hybrid

The exchange rates of the imino protons in the rU-dA hybrid were measured on the singly labeled samples illustrated in Figure 3 and on a triply labeled sample. In the latter sample, the uracils at positions 6, 8, and 9 were labeled with ^{15}N. The resonances of the labeled uracils were observed in the ^{15}N-edited spectrum (Figure 4a), while those of the remaining uracils (i.e., positions 5, 7 and 11) were observed in the ^{14}N-edited spectrum (Figure 4b). This triply labeling strategy allowed us to measure the exchange rates of all uracil imino protons on the same sample.

The exchange rates were measured as a function of the concentration of ammonia (Methods section). The dependence of the exchange rates on the concentration of ammonia base, shown in Figure 5, was analyzed according to the exchange model presented in the Methods section. For all rU-dA base pairs, the exchange is fast even at low ammonia concentrations. As the ammonia concentration is increased, the exchange rates become higher than ~80-90 s^{-1}, and cannot be measured by the NMR transfer of magnetization technique. The equilibrium constants of the base-pair opening reactions were obtained by fitting the exchange rates as a function of ammonia base concentration to Eq. 7 (Methods section). The obtained values are reported in Table 1.

Imino Proton Exchange in the Homologous DNA-DNA Duplex

We have also measured the imino proton exchange in the DNA-DNA duplex with the same base sequence as that of the rU-dA RNA-DNA hybrid (except for the replacement of rU with dT, Figure 6). This duplex, henceforth-abbreviated dT-dA DNA, is of interest because it represents the state of the template when the DNA is not transcribed.

The imino proton resonances of the dT-dA DNA duplex (Figure 6) are well resolved and can be assigned to specific imino protons using standard ^{1}H-^{1}H NOESY experiments. The NOESY spectrum and the resonance assignments for this duplex are discussed in Supplementary Data.

The exchange rates of the imino protons in the dT-dA DNA were measured as a function of the concentration of ammonia under the same experimental conditions as those used for the rU-dA RNA-DNA hybrid. Representative examples of the dependence of the exchange rates on ammonia base concentration are shown in Figure 7. In contrast to the hybrid, the exchange of thymine imino protons in the DNA duplex is slow, i.e., exchange rates less than 10 s^{-1}. The dependence of the exchange rates on ammonia base concentration was analyzed according to Eq. 4 (Methods section). The equilibrium constants for the opening reactions of the dT-dA base pairs in the DNA duplex, obtained from this analysis and Eq. 5, are compared to those of rU-dA base pairs in the RNA-DNA hybrid in Table 1.

Discussion

The results obtained in the present work allow us to define the stability of each base pair in the RNA-DNA and DNA-DNA duplexes investigated. The exchange of an imino proton with solvent protons monitors the conformational transition of the corresponding base pair from its native state inside the double helix to an open, solvent accessible state (Methods section). The equilibrium constant of this opening reaction (K_{op}) provides a measure of the stability of the base pair in its native, intra-helical state. The equilibrium constant K_{op} is related to the free energy change in the opening reaction by

$$\Delta G_{op} = -RT \ln K_{op} \quad (1)$$

where T is the absolute temperature and R is the universal gas constant. Base pairs with high structural stability are characterized by small values of the equilibrium constant K_{op} and large values of the free energy change ΔG_{op}. Alternatively, high K_{op} and small ΔG_{op} values reflect low structural stability of the corresponding base pairs.

The equilibrium constants for the opening of the rU-dA base pairs in the RNA-DNA hybrid range from $9.8 \cdot 10^{-6}$ to $497 \cdot 10^{-6}$ (Table 1). The base pairs in positions 5 through 9 are contiguous in the sequence, while that in position 11 represents a single, isolated rU-dA base pair. It is readily seen that the opening equilibrium constants of the contiguous base pairs are 8-to 50-fold greater than that of the isolated $(rU\text{-}dA)_{11}$ base pair. Accordingly, for these base pairs, the opening free energy changes are smaller than that of $(rU\text{-}dA)_{11}$ by 1.17 to 2.20 kcal/mol. Hence, contiguous rU-dA base pairs are structurally less stable than a rU-dA base pair placed in a mixed sequence context. This finding is in agreement with optical melting studies, which showed that the stability of RNA-DNA hybrid structures containing contiguous rU-dA base pairs is very low.[11] Our results describe this low overall stability at the level of individual rU-dA base pairs. The most stable is the first base pair in the tract, $(rU\text{-}dA)_5$, while the next two base pairs, $(rU\text{-}dA)_6$ and $(rU\text{-}dA)_7$, have the lowest stabilities. For the last base pairs, $(rU\text{-}dA)_8$ and $(rU\text{-}dA)_9$, the stability is increased by ~0.4 kcal/mol relative to that of the preceding two base pairs. This energetic profile of the RNA-DNA hybrid provides new insight into features of transcription termination observed in previous mutational and biochemical studies of the λ tR2 terminator.

The efficiency of transcription termination at the tR2 site is strongly dependent on the rU-dA base pairs in the 2nd to the 5th positions of the tract.[8, 10, 14, 15] Large changes in the efficiency of termination are observed when one or two of these rU-dA base pairs are replaced with rG-dC base pairs. These substitutions also inhibit formation of the hairpin by the upstream inverted sequence in nascent RNA. Our present results suggest that this part of the tract plays such an important functional role due, at least in part, to the structural stability of the base pairs therein. Among all positions in the tract, the rU-dA base pairs in positions 2 to 5 of the tract [i.e., $(rU\text{-}dA)_6$, $(rU\text{-}dA)_7$, $(rU\text{-}dA)_8$ and $(rU\text{-}dA)_9$ in our

construct] have the lowest stabilities (Table 1). Therefore, these base pairs represent the sites of the hybrid where separation of the RNA and DNA strands is energetically least costing. This energetic cost (i.e., 4.3-4.7 kcal/mol) is much less than the costs of opening rU-dA base pairs in mixed sequence contexts (e.g., 6.47 kcal/mol, Table 1) or rG-dC/rC-dG base pairs (i.e., 7.8-9.75 kcal/mol[13]). Hence, substitutions of the rU-dA base pairs in the tract's positions 2 to 5 by stronger base pairs, like in the previous studies, should affect the most the stability of the rU-dA hybrid at the site of transcription termination.

Our proton exchange results reveal that, in addition to low structural stability, the tract of rU-dA base pairs also has unique dynamic properties. These properties are inferred from the observation that the exchange rate of the imino proton in $(rU\text{-}dA)_6$ is the same as the exchange rate of the imino proton in $(rU\text{-}dA)_7$; and the exchange rate of the imino proton in $(rU\text{-}dA)_8$ is the same as the exchange rate of the imino proton in $(rU\text{-}dA)_9$. This observation is presented in Figure 8 by plots of the exchange rates for one base pair against the exchange rates for the other base pair at all concentrations of proton acceptor investigated (similar plots for the other base pairs are given in the Supplementary Data). Both plots in Figure 8 have a slope equal or close to unity indicating that the exchange rates are the same over the entire range of proton acceptor concentrations. This fact explains why the opening equilibrium constant for $(rU\text{-}dA)_6$ is, within experimental errors, the same as that for $(rU\text{-}dA)_7$; and the opening equilibrium constant for $(rU\text{-}dA)_8$ is the same as that for $(rU\text{-}dA)_9$ (Table 1).

In general, in nucleic acid duplexes, imino protons in adjacent base pairs exchange at different rates.[16, 17] This general observation has led to the postulate that base pairs open one at a time, independently of the opening of their neighbors.[16] Our results suggest that, in the rU-dA tract of the RNA-DNA hybrid investigated, some base pairs may not follow this general rule. Instead, it is likely that the exchange of imino protons in $(rU\text{-}dA)_6$ and $(rU\text{-}dA)_7$ occurs in a single opening reaction involving both base pairs. Similarly, for $(rU\text{-}dA)_8$ and $(rU\text{-}dA)_9$, the identity of imino proton exchange rates also suggests concerted opening of the two base pairs. These concerted opening reactions must clearly originate from specific structural features of the tract that couple one base pair to its neighbor. The nature of these structural features is unknown at present. Nevertheless, it is likely that the same structural features aid neighboring bases in the RNA transcript to separate from the DNA template strand in a concerted manner.

Further insight into the energetics of intrinsic transcription termination is provided by our results on the dT-dA DNA duplex (Table 1). The equilibrium constants for opening of the dT-dA base pairs in this duplex are consistently smaller than those of the corresponding rU-dA base pairs in the RNA-DNA hybrid. When the base pair is in a mixed sequence context, like in position 11 of the two duplexes studied here, the K_{op} value for dT-dA is ~ 5-fold lower than that for rU-dA, corresponding to an increase in the opening free energy of 0.9 kcal/mol. Much larger differences are, however, observed for contiguous rU-dA/dT-dA base pairs, namely, the K_{op} values for dT-dA base pairs are 160- to 5,000-fold lower than those for rU-dA base pairs, and the corresponding opening free energies are higher by up to 4.7 kcal/mol. From these energetic profiles (Figure 9a) we conclude that, within the same tract, dT-dA base pairs are much more stable than rU-dA base pairs.

The relevance of our findings for the energetics of transcription termination is best understood in the framework of the thermodynamic model for elongation, termination and editing in transcription, proposed by von Hippel and coworkers.[6, 15, 18] According to this model, formation of the transcription complex from free RNA polymerase and double-stranded DNA is driven by the following free energy change:

$$\Delta G^0_{complex} = \Delta G^0_{DNA-DNA} + \Delta G^0_{RNA-DNA} + \Delta G^0_{NA-polymerse} \quad (2)$$

where $\Delta G^0_{DNA-DNA}$ is the unfavorable free energy change for opening of base pairs in double-stranded DNA to form the transcription bubble; $\Delta G^0_{RNA-DNA}$ is the favorable free energy change for formation of the base pairs in the RNA-DNA hybrid; and the $\Delta G^0_{NA-polymerase}$ term includes the free energies of all interactions of RNA polymerase with the nucleic acid (NA) components of the transcription complex. During elongation, the favorable $\Delta G^0_{RNA-DNA}$ and $\Delta G^0_{NA-polymerase}$ terms outweigh the cost of opening the DNA duplex ($\Delta G^0_{DNA-DNA}$), thus ensuring the processivity of transcription. The model postulates that, at the site of an intrinsic terminator, the favorable interactions between the RNA transcript and the DNA template ($\Delta G^0_{RNA-DNA}$) are weakened, and those between the polymerase and the nucleic acid components ($\Delta G^0_{NA-polymerase}$) are perturbed. As a result, the transcription complex is destabilized so that the RNA-DNA hybrid separates into strands and liberates the newly made RNA, the polymerase is released, and the transcription bubble closes up.

In the framework of this thermodynamic model, our data provide the contribution of each base pair of the double-stranded DNA and of the RNA-DNA hybrid to the destabilization of the elongation complex at the termination site. The contributions are calculated as the total free energy change that occurs when a base pair in the RNA-DNA hybrid opens (or "melts") and the corresponding base pair re-forms in double-stranded DNA:

$$\Delta\Delta G_{op} = \Delta G_{op}(RNA-DNA) - \Delta G_{op}(DNA-DNA) \quad (3)$$

This equation assumes that the presence of the polymerase in the elongation complex does not affect significantly the stabilities of the base pairs in the hybrid structure. The results of the calculations are shown in the last column of Table 1 and in Figure 9b. Clearly, transition of a base pair from the RNA-DNA hybrid to double-stranded DNA is energetically favorable. The free energy change in the transition varies from -0.9 to -4.7 kcal/mol. The smallest free energy contribution is made by the isolated base pair, $(rU\text{-}dA)_{11}$. The most favorable free energy contributions (-3.7 to -4.7 kcal/mol) are made by the base pairs in the 2nd, 3rd and 4th positions in the tract, i.e., $(rU\text{-}dA)_6$, $(rU\text{-}dA)_7$ and $(rU\text{-}dA)_8$. A large contribution from these base pairs is expected since, as discussed above, these are among the weakest base pairs in the hybrid (Figure 9a). One notes also that the contributions of these base pairs are enhanced by the fact that, in the DNA duplex, the corresponding dT-dA base pairs are the most stable base pairs. Hence, these base pairs should experience the largest change in stabilization free energy upon dissociation of the RNA-DNA hybrid and re-formation of double-stranded DNA.

Current molecular models for intrinsic transcription termination attribute the selection of the terminator site by RNA polymerase to the hairpin formed by the inverted GC-rich sequence in nascent RNA, and to the rU-dA hybrid formed when the downstream part of the terminator is transcribed.[8-10, 19] Our present results suggest that the base sequence of the DNA itself could also play a role in the recognition of the termination site by the enzyme. This suggestion is explained in Figure 10. The figure compares the opening free energies (ΔG_{op}) for dT-dA base pairs in two DNA duplexes: (i) the dT-dA DNA duplex studied in the present work, and (ii) a DNA duplex recently studied by our laboratory.[20] The latter duplex (henceforth-abbreviated GC-rich DNA duplex) incorporates in positions 4 through

12 the downstream half of the inverted GC-rich sequence and the first two dT-dA base pairs from the dA-rich sequence of the tR2 site. As one can see, in the GC-rich DNA duplex, the ΔG_{op} values for dT-dA base pairs range from 5.28 to 6.2 kcal/mol. In contrast, in the dT-dA DNA duplex, the ΔG_{op} values are much higher, i. e., 7.4 to 9 kcal/mol. This increase is clearly due to the tract of consecutive dT-dA base pairs in the dT-dA duplex. For example, in the GC-rich duplex, $(dT\text{-}dA)_{11}$ and $(dT\text{-}dA)_{12}$ have opening free energies of 6.2 and 5.28 kcal/mol, respectively. When the same base pairs are placed in the tract of the dT-dA duplex [i.e., $(dT\text{-}dA)_5$ and $(dT\text{-}dA)_6$], their opening free energies become 8.1 and 8.4 kcal/mol, respectively (Table 1). Therefore, when several dT-dA base pairs are consecutive, their stabilities greatly increase relative to that of dT-dA base pairs in a mixed sequence context. Similar energetic features have been previously observed in other DNA tracts of dT-dA base pairs[21-23]. The high stabilities of consecutive dT-dA base pairs could contribute to the recognition of the terminator by the polymerase by increasing the energetic cost for formation of the transcription bubble at this site beyond that required at a site of random base sequence. The high cost of unwinding the DNA helix could, in turn, lower the rate of translocation into the terminator, thus allowing the time necessary for early termination-specific conformational changes in the enzyme and in the RNA to take place.[8, 24]

In summary, the results presented in this paper suggest that an intrinsic transcription terminator uses the same base sequence, i.e., a tract of dA bases in the DNA template strand, to specify termination in two concurrent ways. When the dA bases pair with dT, like in the double-stranded DNA template, the stability of the resulting base pairs is higher than that in a random base sequence. When the dA bases pair with rU, like in the transcription RNA-DNA hybrid, the resulting base pairs are much less stable than those in a hybrid of random sequence. The energetic balance between these alternative paired states of dA bases thus favors the dissociation of the RNA-DNA hybrid as well as the closing of the transcription bubble into a double-stranded DNA helix. Resolution of the structural stability at the level of individual bases also suggests that rU-dA/dT-dA base pairs in the central positions of the dA-rich tract are the main contributors to this energetic balance.

Materials and Methods

Materials

(3-^{15}N)-labeled 2'-*O*-tom-protected uridine phosphoramidite was prepared via a 7-step synthesis as previously described.[25-27] The scheme for this synthesis is shown in Supplementary Data. The labeled phosphoramidite was used to synthesize the RNA strands for the six samples of singly ^{15}N-labeled RNA-DNA hybrid, and for the sample of the triply ^{15}N-labeled RNA-DNA hybrid. The DNA and RNA strands were synthesized on an automated DNA synthesizer using the solid-support phosphoramidite method. They were purified by HPLC on a semipreparative column in 50 mM triethylamine acetate buffer with a gradient of 5%-32% acetonitrile over 46 minutes at 60 °C. The RNA strand containing ^{15}N-guanine (Cambridge Isotope Laboratory, MA) was synthesized by *in vitro* transcription using T7 RNA polymerase.[28] For both DNA and RNA strands the counterions were replaced with Na^+ ions by repeated centrifugation in Amicon Ultra-4 centrifugal filter units using 0.5 M NaCl, followed by centrifugation against water. The final NMR samples contained 0.3 to 0.8 mM RNA-DNA or DNA-DNA duplex in 10 mM Na_2HPO_4/NaH_2PO_4 and 0.5 mM EDTA in 90% H_2O/10% D_2O at pH 7.8 ± 0.1 (at 10 °C). All samples also contained 0.5 mM triethanolamine, which was used to determine the pH of the samples directly in the NMR tube as we have described.[29]

Methods

NMR Experiments—The NMR experiments were performed at 10 °C on a Varian INOVA 500 spectrometer operating at 11.75 T. The exchange rates of imino protons were measured by transfer of magnetization from water. The water resonance was selectively inverted using a Gaussian 180 pulse (5.8ms) followed by a variable delay for the exchange of magnetization between water and imino protons. A gradient of 0.21 G/cm was applied during the exchange delay to prevent the effects of radiation damping upon the recovery of water magnetization to equilibrium. A second selective pulse on water was applied to bring the water magnetization back onto the z-axis before observation. Twenty-five values of the exchange delay in the range from 1 to 800 ms were used in each experiment. The exchange rates were calculated from the dependence of the intensity of the imino proton resonance on the exchange delay as described previously.[17] For the unlabeled samples the observation was with the Jump-and-Return pulse sequence.[30] For the ^{15}N-labeled samples the observation was with the one-dimensional version of the fast HSQC (fHSQC) pulse sequence to edit the resonances of protons attached to ^{15}N and eliminate all other proton resonances.[31] A modified, ^{14}N-editing, fHSQC pulse sequence was used to filter out the resonances of protons attached to ^{15}N and retain all other proton resonances.[32] The highest exchange rates that can be accurately measured by these methods is ~80 - 90 s^{-1}. The ^{1}H-^{1}H NOESY spectra were obtained using the Watergate pulse sequence[33] with a mixing time of 250 ms.

Imino Proton Exchange in Nucleic Acid Duplexes—The exchange of imino protons in nucleic acids is a two-step process. In the first step, the hydrogen bonds in the base pair break and the base flips out of the structure into an open state. In this state, the imino proton is accessible to proton acceptors present in the solvent. The second step is the actual transfer of the proton to an acceptor, for example, NH_3. The exchange rate observed experimentally is given as:[16, 34]

$$k_{ex} = \frac{k_{op} k_B [B]}{k_{cl} + k_B \cdot [B]} \quad (4)$$

where k_{op} and k_{cl} are the rates of opening and closing, respectively, of the base containing the imino proton, [B] is the concentration of proton acceptor B, and k_B is the rate constant for the transfer of the imino proton to the proton acceptor in isolated nucleotides. The rates of opening and closing define the equilibrium constant of the opening reaction:

$$K_{op} = \frac{k_{op}}{k_{cl}} \quad (5)$$

Two kinetic regimes for imino proton exchange can be distinguished depending on how the rate of exchange from the open state compares with the rate of closing. When the concentration of proton acceptor is sufficiently high to make the exchange from the open state very fast ($k_{ex,open} \gg k_{cl}$, EX1 regime), the exchange is limited by the rate of base-pair opening. In this case, Eq. 4 becomes:

$$k_{ex} = k_{op} \quad (6)$$

At low concentrations of proton acceptor, the rate of exchange from the open state is much smaller than the rate of base-pair closing ($k_{ex,open} \ll k_{cl}$, EX2 regime). In this regime, the observed exchange rate is proportional to the concentration of proton acceptor:

$$k_{ex}=K_{op}k_B[B] \quad (7)$$

In this work, we have used ammonia base (NH_3) as the imino proton acceptor in the exchange. Previous work from this and other laboratories has shown that, due to its small size, good solubility, high p*K*, and lack of charge, ammonia base is the acceptor of choice for proton exchange studies of nucleic acids.[16, 17] The rate constants for transfer of imino protons to NH_3 (k_B) were previously calculated as: 8.8×10^8 $M^{-1}s^{-1}$ for the uracil proton and 4.1×10^8 $M^{-1}s^{-1}$ for the thymine proton, at 10 °C.[13] The total ammonia concentration was varied from 0 to 150 mM for the experiments on the rU-dA RNA-DNA hybrid, and from 0 to 500 mM for the experiments on the dT-dA DNA duplex. The concentration of ammonia base NH_3 was calculated from the total ammonia concentration C_0 and the pH as:

$$[B]=C_0 \times 10^{-pK}/(10^{-pH}+10^{-pK}) \quad (8)$$

The pH was measured at each ammonia concentration, directly in the NMR tube, using the proton resonances of triethanolamine.[29] The p*K* value of ammonia at 10 °C is 9.73.[35]

Supplementary Material

Refer to Web version on PubMed Central for supplementary material.

Acknowledgments

This work was supported by a grant from the National Institutes of Health (GM077188). We would like to thank Dr. Smita Patel (University of Medicine and Dentistry of New Jersey-Robert Wood Johnson Medical School) for a gift of T7 RNA polymerase, and Dr. Michael Calter (Wesleyan University) for his help with the synthesis of (3-^{15}N)-labeled 2'-O-tom protected uridine phosphoramidite.

References

1. Nudler E, Mustaev A, Lukhtanov E, Goldfarb A. The RNA-DNA Hybrid Maintains the Register of Transcription by Preventing Backtracking of RNA Polymerase. Cell 1997;89:33–41. [PubMed: 9094712]
2. Korzheva N, Mustaev A, Kozlov M, Malhotra A, Nikiforov V, Goldfarb A, Darst SA. A Structural Model of Transcription Elongation. Science 2000;289:619–625. [PubMed: 10915625]
3. Lesnik EA, Sampath R, Levene HB, Henderson TJ, McNeil JA, Ecker DJ. Prediction of rho-independent transcriptional terminators in *Escherichia Coli*. Nucleic Acids Res 2001;29:3583–3594. [PubMed: 11522828]
4. d'Aubenton Carafa Y, Brody E, Thermes C. Prediction of Rho-independent Escherichia coli Transcription Terminators. A Statistical Analysis of their RNA Stem-Loop Structures. J Mol Biol 1990;216:835–858. [PubMed: 1702475]
5. Yarnell WS, Roberts JW. Mechanism of Intrinsic Transcription Termination and Antitermination. Science 1999;284:611–615. [PubMed: 10213678]
6. von Hippel PH. An Integrated Model of the Transcription Complex in Elongation, Termination, and Editing. Science 1998;281:660–665. [PubMed: 9685251]
7. Greive SJ, von Hippel PH. Thinking quantitatively about transcription regulation. Nature Rev Mol Cell Biol 2005;6:221–232. [PubMed: 15714199]
8. Gusarov I, Nudler E. The Mechanism of Intrinsic Transcription Termination. Mol Cell 1999;3:495–504. [PubMed: 10230402]
9. Nudler E, Gottesman ME. Transcription termination and anti-termination in *E. Coli*. Genes Cells 2002;7:755–768. [PubMed: 12167155]

10. Komissarova N, Becker J, Solter S, Kireeva M, Kashlev M. Shortening of RNA:DNA Hybrid in the Elongation Complex of RNA Polymerase Is a Prerequisite for Transcription Termination. Mol Cell 2002;10:1151–1162. [PubMed: 12453422]
11. Martin FH, Tinoco IJ. RNA-DNA hybrid duplexes containing oligo (dA:rU) sequences are exceptionally unstable and may facilitate termination of transcription. Nucleic Acids Res 1980;8:2295–2299. [PubMed: 6159577]
12. Wilson KS, von Hippel PH. Transcription termination at intrinsic terminators: The role of the RNA hairpin. Proc Natl Acad Sci US 1995;92:8793–8797.
13. Huang Y, Chen C, Russu IM. Dynamics and Stability of Individual Base Pairs in Two Homologous RNA-DNA Hybrids. Biochemistry 2009;48:3988–3997. [PubMed: 19296713]
14. Epshtein V, Cardinale CJ, Ruckenstein AE, Borukhov S, Nudler E. An Alosteric Path to Transcription Termination. Mol Cell 2007;28:991–1001. [PubMed: 18158897]
15. Datta K, von Hippel PH. Direct Spectroscopic Study of Reconstituted Transcription Complexes Reveals That Intrinsic Termination is Driven Primarily by Thermodynamic Destabilization of the Nucleic Acid Framework. J Biol Chem 2008;283:3537–3549. [PubMed: 18070878]
16. Gueron M, Leroy J-L. Studies of Base Pair Kinetics by NMR Measurement of Proton Exchange. Methods Enzymol 1995;261:383–413. [PubMed: 8569504]
17. Russu IM. Probing Site-Specific Energetics in Proteins and Nucleic Acids by Hydrogen Exchange and NMR Spectroscopy. Methods Enzymol 2004;379:152–175. [PubMed: 15051357]
18. Yager TD, von Hippel PH. A Thermodynamic Analysis of RNA Transcript Elongation and Termination in *Escherichia coli*. Biochemistry 1991;30:1097–1118. [PubMed: 1703438]
19. Toulokhonov I, Artsimovitch I, Landick R. Allosteric control of RNA polymerase by a site that contacts nascent RNA hairpins. Science 2001;292:730–733. [PubMed: 11326100]
20. Huang Y, Weng X, Russu IM. In preparation. 2010
21. Leroy JL, Charretier E, Kochoyan M, Gueron M. Evidence from Base-Pair Kinetics for Two Types of Adenine Tract Structures in Solution: Their Relation to DNA Curvature. Biochemistry 1988;27:8894–8898. [PubMed: 3233210]
22. Moe JG, Russu IM. Proton Exchange and Base Pair Opening Kinetics in 5′-d (CGCGAATTCGCG)-3′ and Related Dodecamers. Nucleic Acids Res 1990;18:821–827. [PubMed: 2156233]
23. Moe JG, Folta-Stogniew E, Russu IM. Energetics of Base-Pair Opening in a DNA Dodecamer Containing an A_3T_3 Tract. Nucleic Acids Res 1995;23:1984–1989.
24. Tadigotla VR, Maoileidigh DO, Sengupta AM, Epshtein V, Ebright RH, Nudler E, Ruckenstein AE. Thermodynamic and kinetic modeling of transcriptional pausing. Proc Natl Acad Sci U S A 2006;103:4439–4444. [PubMed: 16537373]
25. Ariza X, Bou V, Vilarrasa J. A new Route to ^{15}N-labeled, N-alkyl, and N-Amino Nucleosides via N-Nitration of Uridines and Inosines. J Am Chem Soc 1995;117:3665–3673.
26. Pitsch S, Weiss PA, Jenny L, Stutz A, Wu XL. Reliable chemical synthesis of oligoribonucleotides (RNA) with 2′-O-[(triisopropylsilyl)oxy]methyl(2′-O-tom)-protected phosphoramidites. Helvetica Chimica Acta 2001;84:3773–3795.
27. Wenter P, Pitsch S. Synthesis of selectively ^{15}N-labeled 2′-O-{[(triisopropylsilyl)oxy]methyl} (=tom)-protected ribonucleoside phosphoramidites and their incorporation into a bistable 32mer RNA sequence. Helvetica Chimica Acta 2003;86:3955–3974.
28. Milligan JF, Groebe DR, Witherell GW, Uhlenbeck OC. Oligoribonucleotide synthesis using T7 RNA polymerase and synthetic DNA templates. Nucleic Acids Res 1987;15:8783–8798. [PubMed: 3684574]
29. Chen C, Russu IM. Sequence-Dependence of the Energetics of Opening of AT Base Pairs in DNA. Biophys J 2004;87:1–7.
30. Plateau P, Gueron M. Exchangeable proton NMR without base-line distortion, using new strong-pulse sequences. J Am Chem Soc 1982;104:7310–7311.
31. Mori S, Abeygunawardana C, Johnson MO, van Zijl PCM. Improved Sensitivity of HSQC Spectra of Exchanging Protons at Short Interscan Delays Using a new Fast HSQC(FHSQC) Detection Scheme That Avoids Water Saturation. J Magn Reson B 1995;108:94–98. [PubMed: 7627436]

32. Chen C, Jiang L, Michalczyk R, Russu IM. Structural Energetics and Base-Pair Opening Dynamics in Sarcin-Ricin Domain RNA. Biochemistry 2006;45:13606–13613. [PubMed: 17087514]
33. Lippens G, Dhalluin C, Wieruszeski J-M. Use of a water flip-back pulse in the homonuclear NOESY experiment. J Biomol NMR 1995;5:327–331.
34. Englander SW, Kallenbach NR. Hydrogen exchange and structural dynamics of proteins and nucleic acids. Q Rev Biophys 1984;16:521–655. [PubMed: 6204354]
35. Weast, RC. CRC Handbook of Chemistry and Physics. 67. CRC Press; Boca Raton, FL: 1987.

(a)

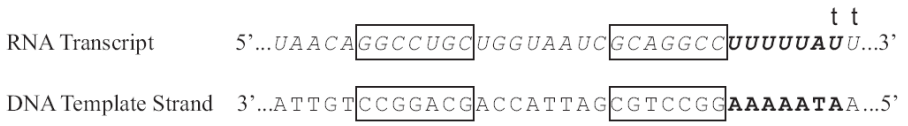

(b)

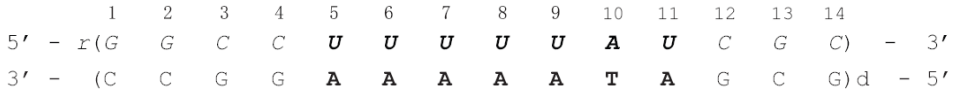

(c)

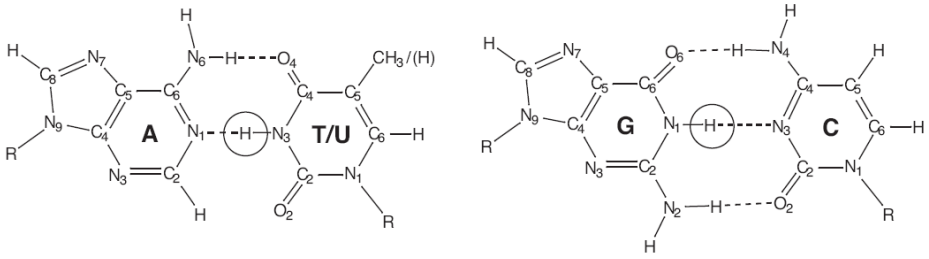

Figure 1.

(a) Base sequences of the DNA template strand and of the RNA transcript in tR2 transcription termination site from bacteriophage λ. The GC-rich sequence with inverted symmetry is boxed. The sequences corresponding to the A-rich tract are shown in bold. Transcription terminates at one of the two positions indicated by a "t". The most frequent termination point is at the first of these positions.

(b) Base sequence and numbering of base pairs in the RNA-DNA hybrid investigated.

(c) The structures of GC and AU/T base pairs with the imino protons highlighted.

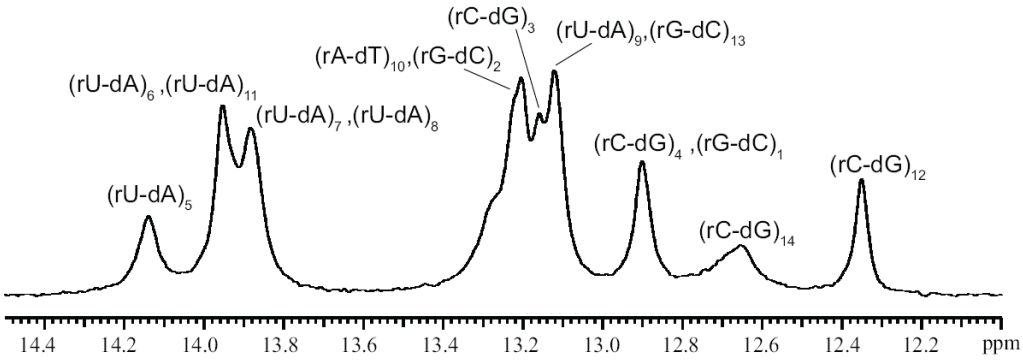

Figure 2.
Imino proton resonances of the rU-dA RNA-DNA hybrid in 10 mM phosphate buffer at pH 7.8 and at 10°C.

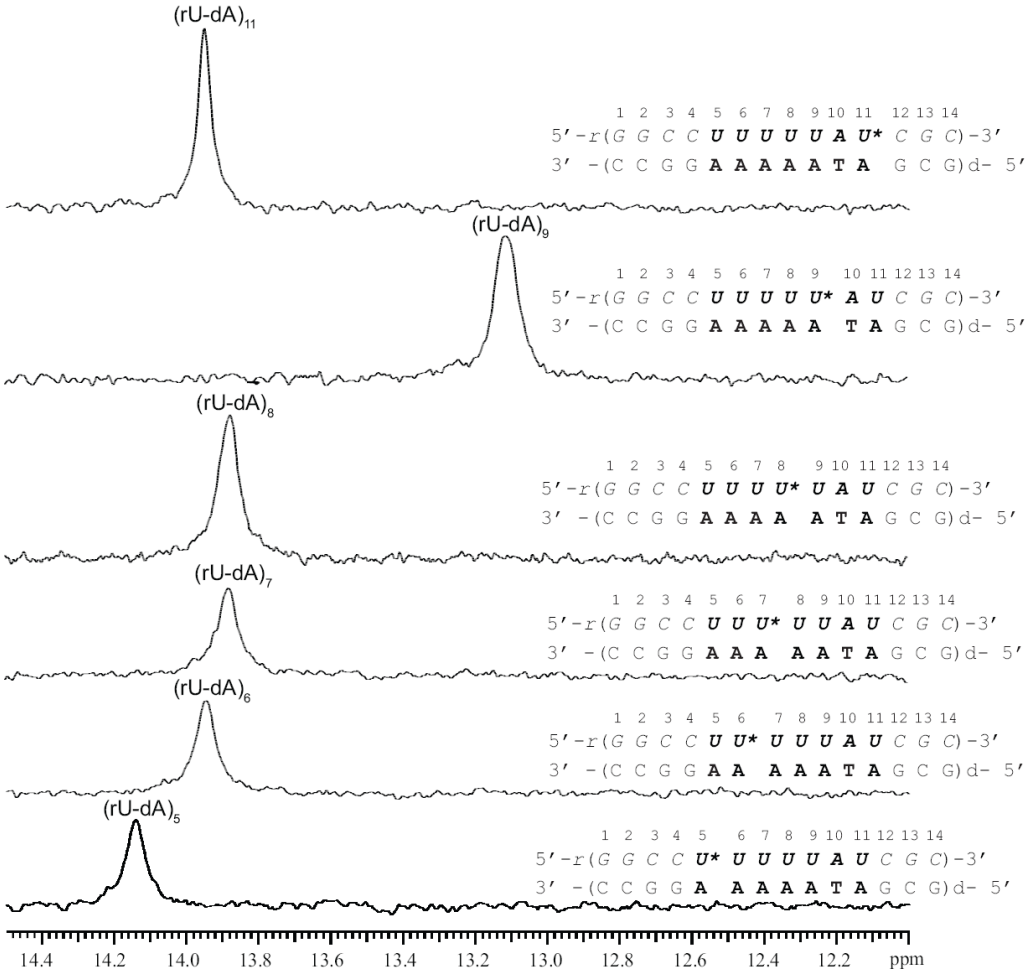

Figure 3.

^{15}N-edited NMR resonances of imino protons for rU-dA RNA-DNA hybrid molecules in which a single uracil was labeled with ^{15}N. The ^{15}N-labeled uracil in each molecule is indicated by an asterisk.

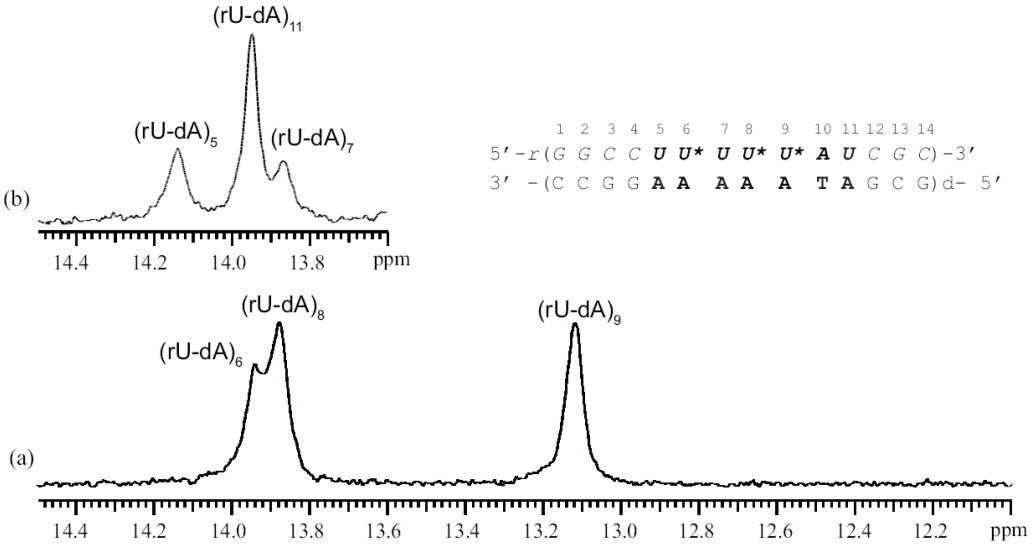

Figure 4.

NMR resonances of the uracil imino protons for the rU-dA RNA-DNA hybrid containing ^{15}N-labeled uracil in positions 6, 8 and 9. (a) ^{15}N-edited uracil imino proton resonances. (b) ^{14}N-edited uracil imino proton resonances.

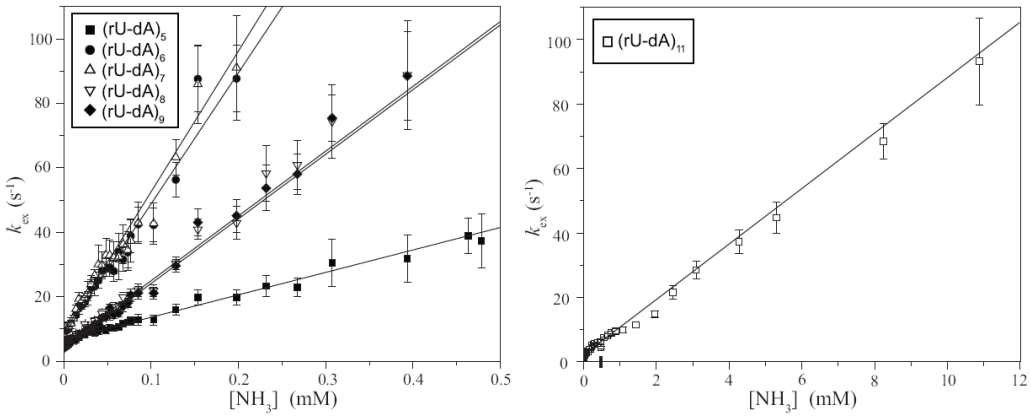

Figure 5.

Dependence of the exchange rates of individual uracil imino protons in the rU-dA RNA-DNA hybrid on the concentration of ammonia base. The exchange rates for $(rU\text{-}dA)_{11}$ are shown separately due to the different range of ammonia base concentrations in which the exchange can be measured. The lines represent least-squares fits to Eq. 7.

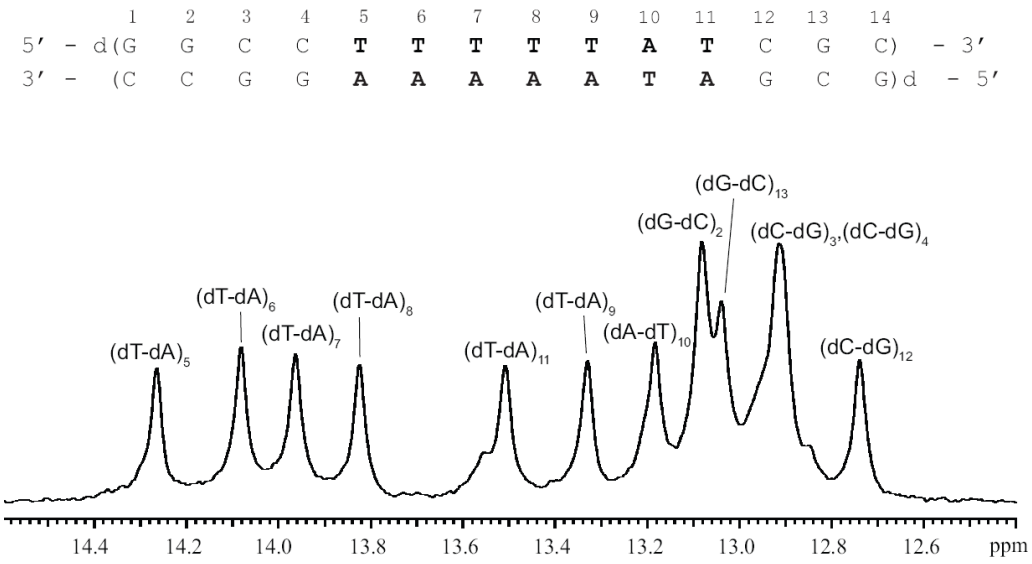

Figure 6.

The base sequence and the imino proton resonances of the dT-dA DNA duplex in 10 mM phosphate buffer at pH 7.8 and at 10°C.

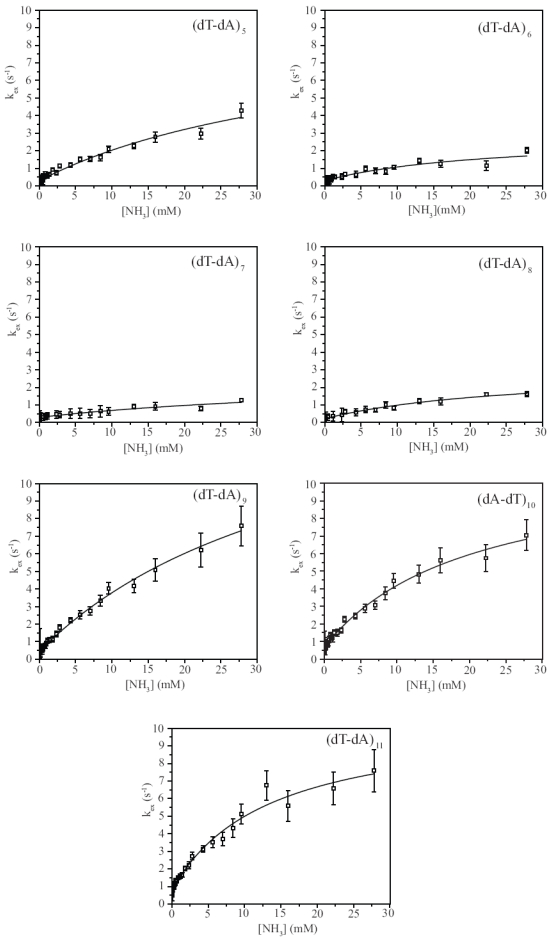

Figure 7.

Dependence of the exchange rates of thymine imino protons in the dT-dA DNA duplex on the concentration of ammonia base. The curves represent nonlinear least-squares fits to Eq. 4.

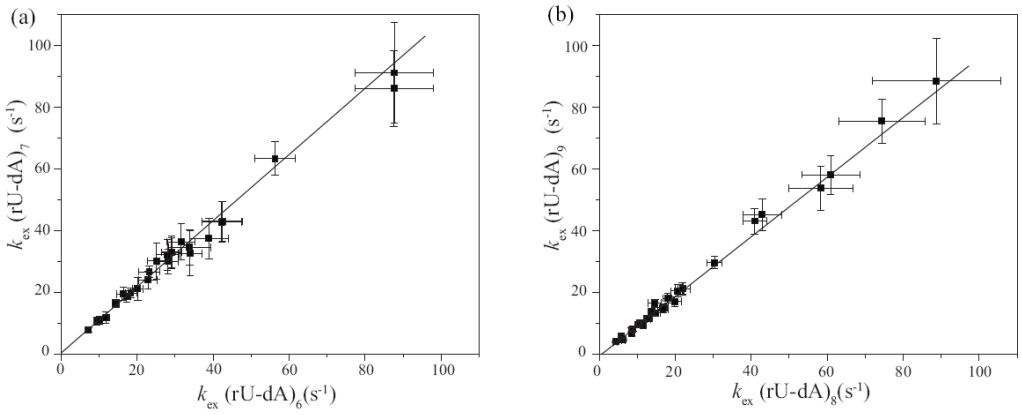

Figure 8.

(a) Comparison of the exchange rates of the imino proton in $(rU\text{-}dA)_7$ to the exchange rates of the imino proton in $(rU\text{-}dA)_6$; the slope of the least-squares fitted line is 1.07±0.02.
(b) Comparison of the exchange rates of the imino proton in $(rU\text{-}dA)_9$ to the exchange rates of the imino proton in $(rU\text{-}dA)_8$; the slope of the least-squares fitted line is 0.97±0.03.

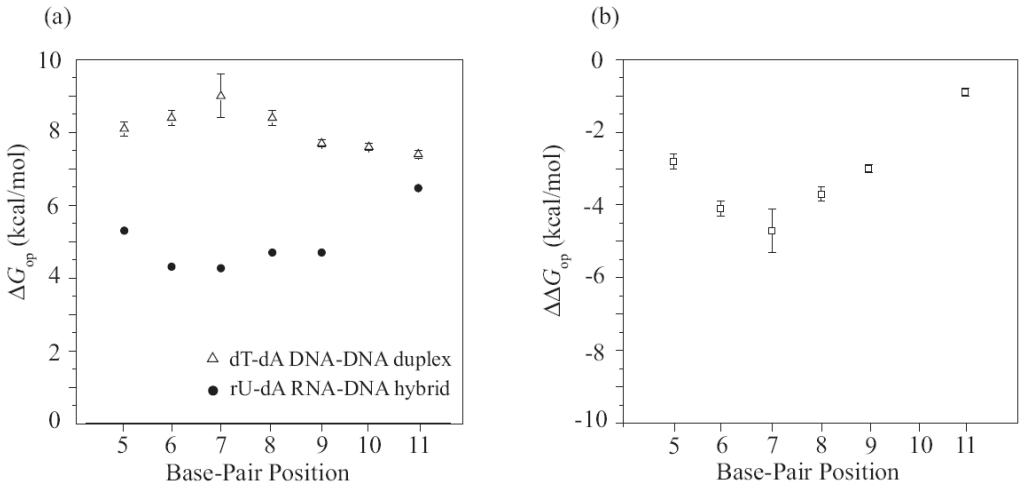

Figure 9.

(a) Opening free energy changes (ΔG_{op}) for rU-dA/dT-dA base pairs in the RNA-DNA and DNA-DNA duplexes investigated. The experimental errors for the values in the RNA-DNA hybrid are smaller than the symbols.

(b) The free energy contributions ($\Delta\Delta G_{op}$) of individual rU-dA/dT-dA base pairs to the destabilization of the elongation complex at the transcription termination site, calculated based on the thermodynamic model (Eq. 3).

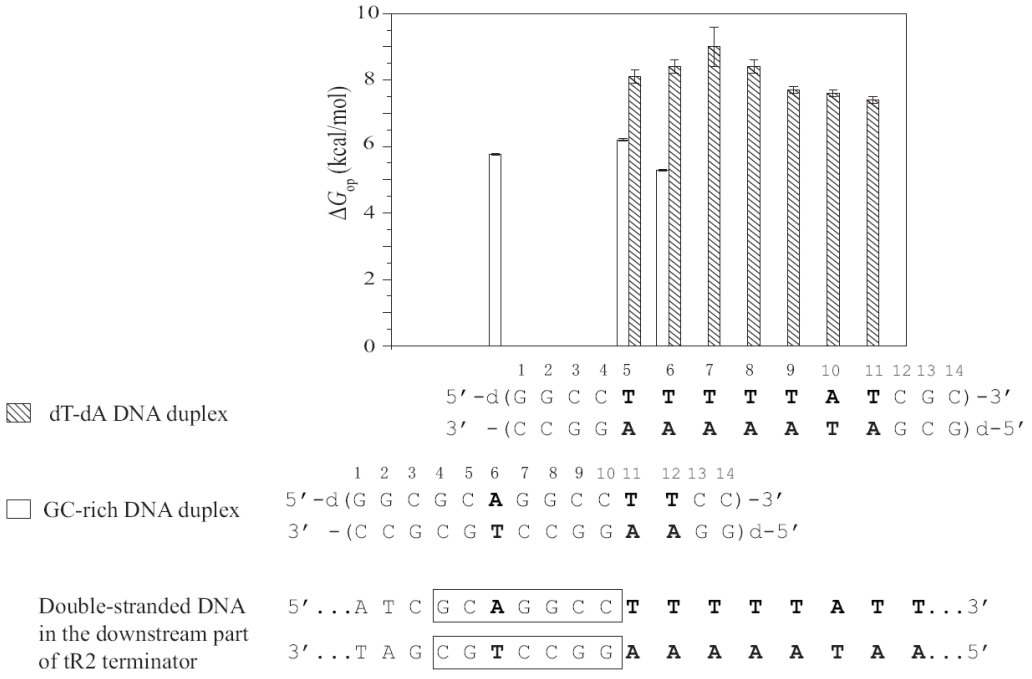

Figure 10.

Opening free energy changes (ΔG_{op} in kcal/mol at 10°C) for dT-dA base pairs in the GC-rich and dT-dA DNA duplexes. Empty bars represent the values in the GC-rich duplex, and filled bars represent the values in the dT-dA duplex. The downstream part of the double-stranded DNA in the tR2 terminator is shown at the bottom.

Table 1

Equilibrium Constants and Free Energy Changes for Base-Pair Opening in the rU-dA RNA-DNA Hybrid and dT-dA DNA Duplexes Investigated

rU-dA RNA-DNA Hybrid			dT-dA DNA Duplex			
Base pair	**K_{op} (×10^6)**	**ΔG_{op}[a]**	**Base pair**	**K_{op} (×10^6)**	**ΔG_{op}[a]**	**$\Delta\Delta G_{op}$[a]**
$(rU\text{-}dA)_5$	79 ± 2	5.30±0.01	$(dT\text{-}dA)_5$	0.5±0.2	8.1±0.2	-2.8±0.2
$(rU\text{-}dA)_6$	462 ± 14	4.31±0.02	$(dT\text{-}dA)_6$	0.3±0.1	8.4±0.2	-4.1±0.2
$(rU\text{-}dA)_7$	497 ± 19	4.27±0.02	$(dT\text{-}dA)_7$	0.1±0.1	9.0±0.6	-4.7±0.6
$(rU\text{-}dA)_8$	228 ± 7	4.70±0.02	$(dT\text{-}dA)_8$	0.3±0.1	8.4±0.2	-3.7±0.2
$(rU\text{-}dA)_9$	228 ± 5	4.70±0.01	$(dT\text{-}dA)_9$	1.0±0.2	7.7±0.1	-3.0±0.1
$(rA\text{-}dT)_{10}$	b	b	$(dA\text{-}dT)_{10}$	1.4±0.2	7.6±0.1	
$(rU\text{-}dA)_{11}$	9.8 ± 0.4	6.47±0.02	$(dT\text{-}dA)_{11}$	1.9±0.3	7.4±0.1	-0.9±0.1

[a] in kcal/mol at 10°C

[b] Imino proton resonance is not resolved in the NMR spectrum